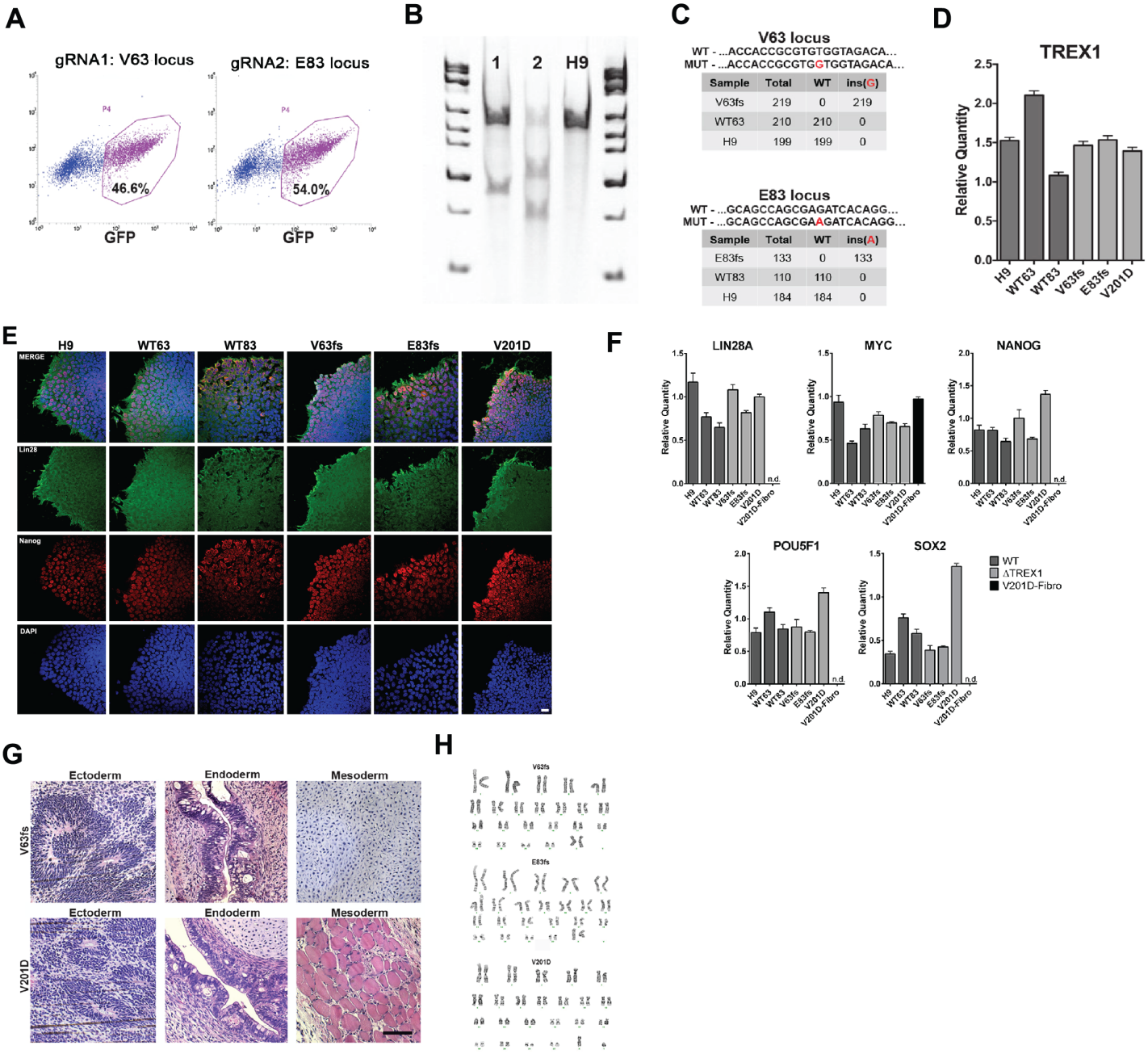
A
gRNA1: V63 locus
gRNA2: E83 locus
P4
46.6%
54.0%
GFP
B
1
2
H9
C
V63 locus
WT - ...ACCACCGCGTGTGGTAGACA...
MUT - ...ACCACCGCGTGGTGGTAGACA...
Sample | Total | WT | ins(G)
V63fs | 219 | 0 | 219
WT63 | 210 | 210 | 0
H9 | 199 | 199 | 0
E83 locus
WT - ...GCAGCCAGCGAGATCACAGG...
MUT - ...GCAGCCAGCGAAGATCACAGG...
Sample | Total | WT | ins(A)
E83fs | 133 | 0 | 133
WT83 | 110 | 110 | 0
H9 | 184 | 184 | 0
D
TREX1
Relative Quantity
H9
WT63
WT83
V63fs
E83fs
V201D
E
H9
WT63
WT83
V63fs
E83fs
V201D
MERGE
Lin28
Nanog
DAPI
F
LIN28A
MYC
NANOG
POU5F1
SOX2
Relative Quantity
n.d
WT
ΔTREX1
V201D-Fibro
G
Ectoderm
Endoderm
Mesoderm
V63fs
V201D
H
V63fs
E83fs
V201D

Figure S1

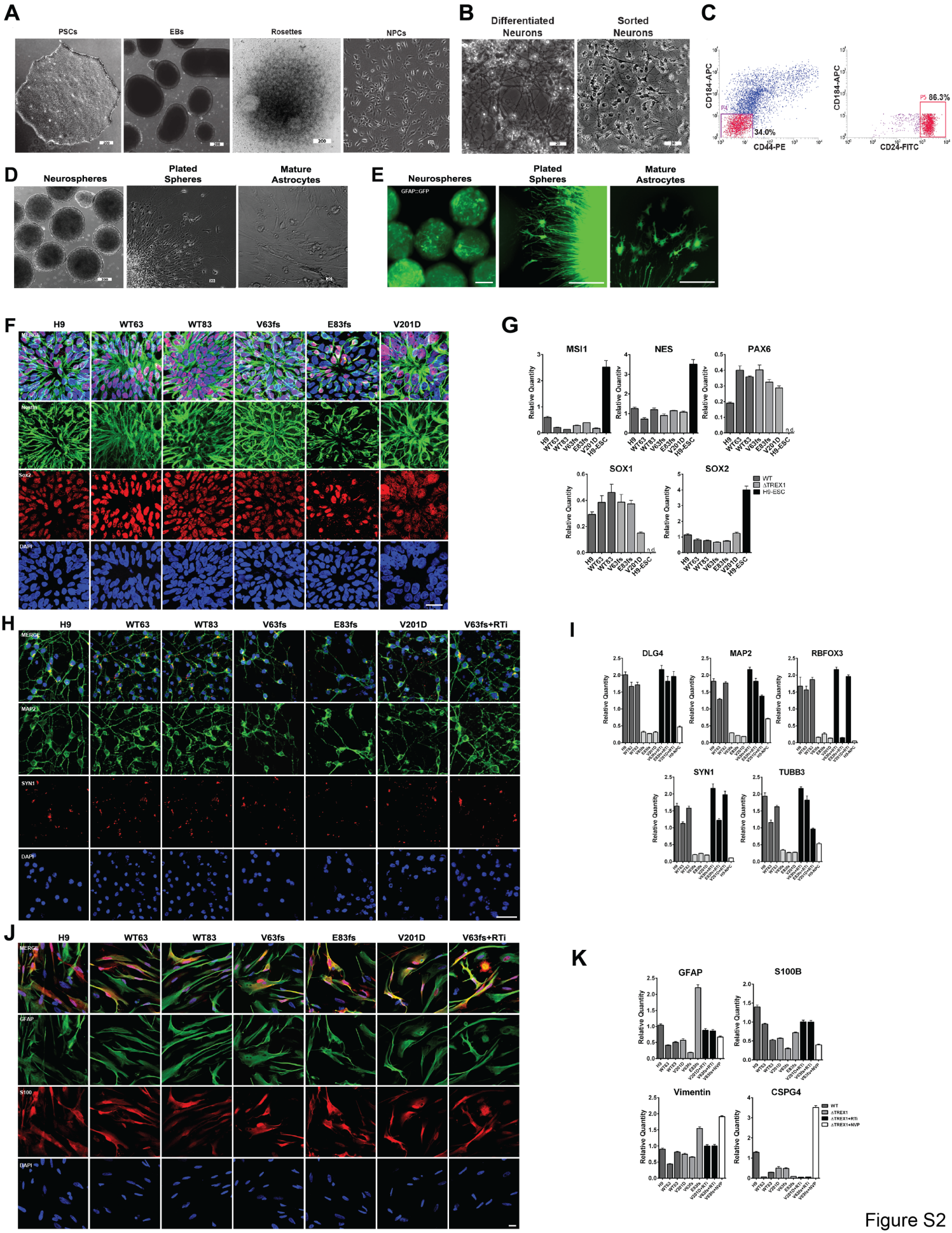
A
PSCs
EBs
Rosettes
NPCs
B
Differentiated Neurons
Sorted Neurons
C
CD184-APC
CD44-PE
34.0%
P4
CD24-FITC
86.3%
P5
D
Neurospheres
Plated Spheres
Mature Astrocytes
E
Neurospheres
GFAP::GFP
Plated Spheres
Mature Astrocytes
F
H9
WT63
WT83
V63fs
E83fs
V201D
MERGE
Nestin
Sox2
DAPI
G
MSI1
NES
PAX6
SOX1
SOX2
Relative Quantity
H9
WT63
WT83
V63fs
E83fs
V201D
H9-ESC
n.d.
WT
ΔTREX1
H9-ESC
H
V63fs+RTi
MERGE
MAP2
SYN1
DAPI
I
DLG4
MAP2
RBFOX3
SYN1
TUBB3
J
GFAP
S100
K
GFAP
S100B
Vimentin
CSPG4
ΔTREX1+RTi
ΔTREX1+NVP

Figure S2

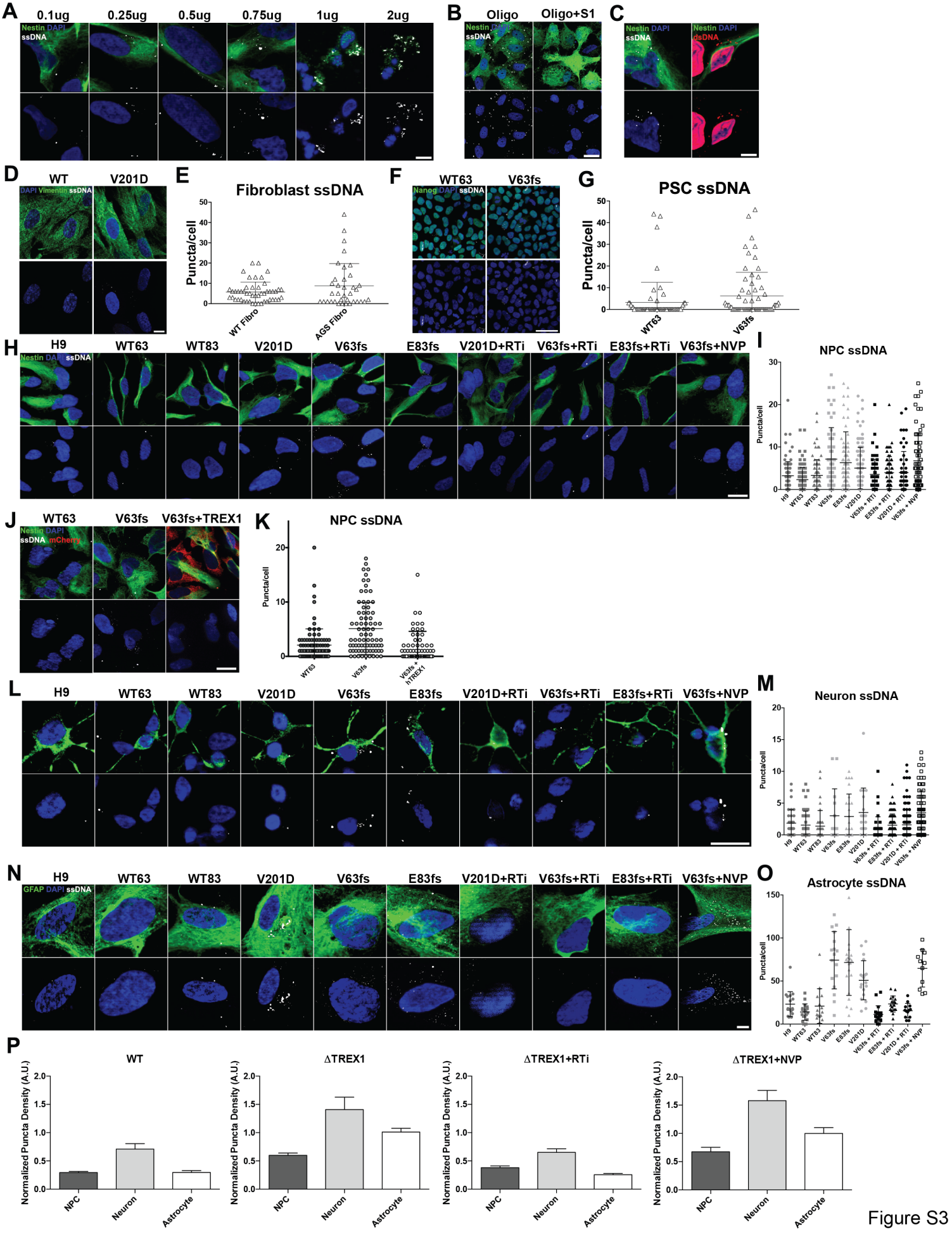
A
0.1ug
0.25ug
0.5ug
0.75ug
1ug
2ug
Nestin DAPI ssDNA
B
Oligo
Oligo+S1
C
Nestin DAPI dsDNA
D
WT
V201D
DAPI Vimentin ssDNA
E
Fibroblast ssDNA
Puncta/cell
WT Fibro
AGS Fibro
F
WT63
V63fs
Nanog DAPI ssDNA
G
PSC ssDNA
H
H9
WT63
WT83
V201D
V63fs
E83fs
V201D+RTi
V63fs+RTi
E83fs+RTi
V63fs+NVP
I
NPC ssDNA
J
V63fs+TREX1
Nestin DAPI ssDNA mCherry
K
L
M
Neuron ssDNA
N
GFAP DAPI ssDNA
O
Astrocyte ssDNA
P
WT
ΔTREX1
ΔTREX1+RTi
ΔTREX1+NVP
Normalized Puncta Density (A.U.)
NPC
Neuron
Astrocyte

Figure S3

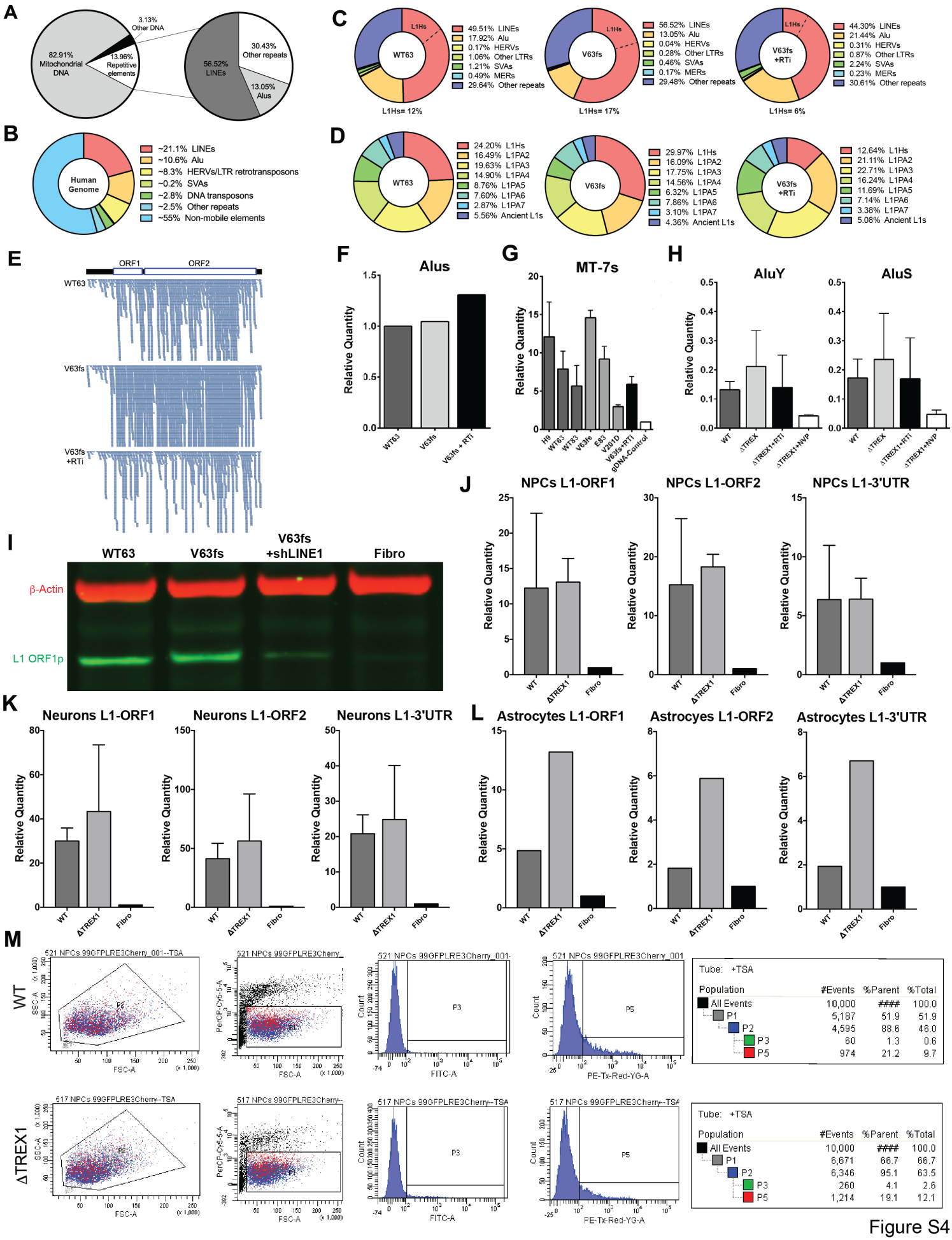
A
3.13% Other DNA
82.91% Mitochondrial DNA
13.96% Repetitive elements
56.52% LINEs
30.43% Other repeats
13.05% Alus
B
Human Genome
~21.1% LINEs
~10.6% Alu
~8.3% HERVs/LTR retrotransposons
~0.2% SVAs
~2.8% DNA transposons
~2.5% Other repeats
~55% Non-mobile elements
C
WT63
L1Hs
49.51% LINEs
17.92% Alu
0.17% HERVs
1.06% Other LTRs
1.21% SVAs
0.49% MERs
29.64% Other repeats
L1Hs= 12%
V63fs
56.52% LINEs
13.05% Alu
0.04% HERVs
0.28% Other LTRs
0.46% SVAs
0.17% MERs
29.48% Other repeats
L1Hs= 17%
V63fs +RTi
44.30% LINEs
21.44% Alu
0.31% HERVs
0.87% Other LTRs
2.24% SVAs
0.23% MERs
30.61% Other repeats
L1Hs= 6%
D
WT63
24.20% L1Hs
16.49% L1PA2
19.63% L1PA3
14.90% L1PA4
8.76% L1PA5
7.60% L1PA6
2.87% L1PA7
5.56% Ancient L1s
V63fs
29.97% L1Hs
16.09% L1PA2
17.75% L1PA3
14.56% L1PA4
6.32% L1PA5
7.86% L1PA6
3.10% L1PA7
4.36% Ancient L1s
V63fs +RTi
12.64% L1Hs
21.11% L1PA2
22.71% L1PA3
16.24% L1PA4
11.69% L1PA5
7.14% L1PA6
3.38% L1PA7
5.08% Ancient L1s
E
ORF1
ORF2
WT63
V63fs
V63fs +RTi
F
Alus
Relative Quantity
WT63
V63fs
V63fs + RTi
G
MT-7s
Relative Quantity
H9
WT63
WT83
V63fs
E83
V701D
V63fs+RTi
gDNA-Control
H
AluY
AluS
Relative Quantity
WT
ΔTREX
ΔTREX1+RTi
ΔTREX1+NVP
I
WT63
V63fs
V63fs +shLINE1
Fibro
β-Actin
L1 ORF1p
J
NPCs L1-ORF1
NPCs L1-ORF2
NPCs L1-3'UTR
Relative Quantity
WT
ΔTREX1
Fibro
K
Neurons L1-ORF1
Neurons L1-ORF2
Neurons L1-3'UTR
Relative Quantity
WT
ΔTREX1
Fibro
L
Astrocytes L1-ORF1
Astrocyes L1-ORF2
Astrocytes L1-3'UTR
Relative Quantity
WT
ΔTREX1
Fibro
M
WT
521 NPCs 99GFPLRE3Cherry_001--TSA
521 NPCs 99GFPLRE3Cherry
521 NPCs 99GFPLRE3Cherry_001
521 NPCs 99GFPLRE3Cherry_001
SSC-A
FSC-A
PerCP-Cy5-5-A
Count
FITC-A
PE-Tx-Red-YG-A
P1
P2
P3
P5
Tube: +TSA
Population #Events %Parent %Total
All Events 10,000 #### 100.0
P1 5,187 51.9 51.9
P2 4,595 88.6 46.0
P3 60 1.3 0.6
P5 974 21.2 9.7
ΔTREX1
517 NPCs 99GFPLRE3Cherry--TSA
517 NPCs 99GFPLRE3Cherry--
517 NPCs 99GFPLRE3Cherry--TSA
517 NPCs 99GFPLRE3Cherry--TSA
Tube: +TSA
Population #Events %Parent %Total
All Events 10,000 #### 100.0
P1 6,671 66.7 66.7
P2 6,346 95.1 63.5
P3 260 4.1 2.6
P5 1,214 19.1 12.1

Figure S4

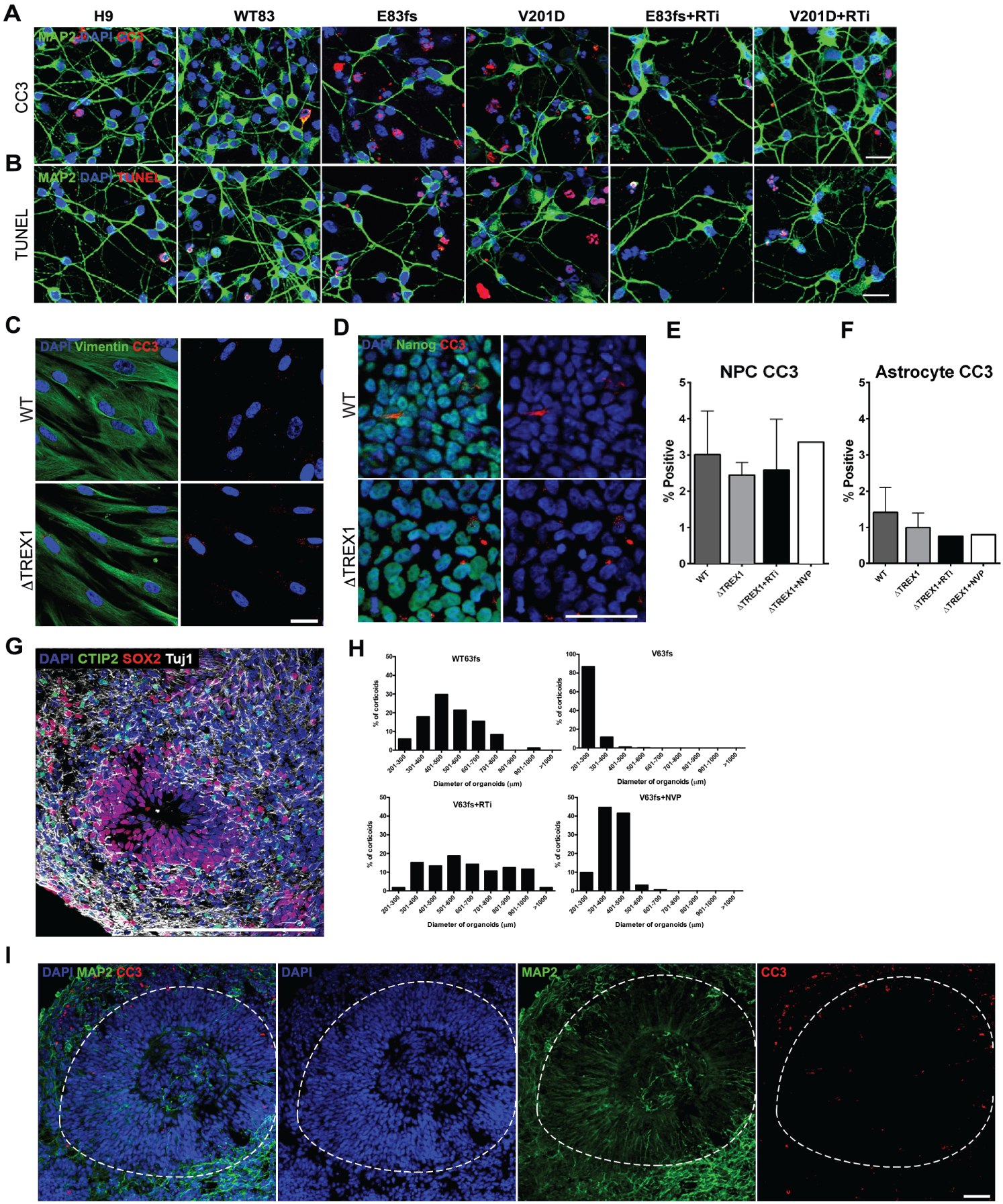
A
H9
WT83
E83fs
V201D
E83fs+RTi
V201D+RTi
MAP2 DAPI CC3
CC3
B
MAP2 DAPI TUNEL
TUNEL
C
DAPI Vimentin CC3
WT
ΔTREX1
D
DAPI Nanog CC3
WT
ΔTREX1
E
NPC CC3
% Positive
WT
ΔTREX1
ΔTREX1+RTi
ΔTREX1+NVP
F
Astrocyte CC3
% Positive
WT
ΔTREX1
ΔTREX1+RTi
ΔTREX1+NVP
G
DAPI CTIP2 SOX2 Tuj1
H
WT63fs
V63fs
V63fs+RTi
V63fs+NVP
% of corticoids
Diameter of organoids (μm)
201-300
301-400
401-500
501-600
601-700
701-800
801-900
901-1000
>1000
I
DAPI MAP2 CC3
DAPI
MAP2
CC3

Figure S5

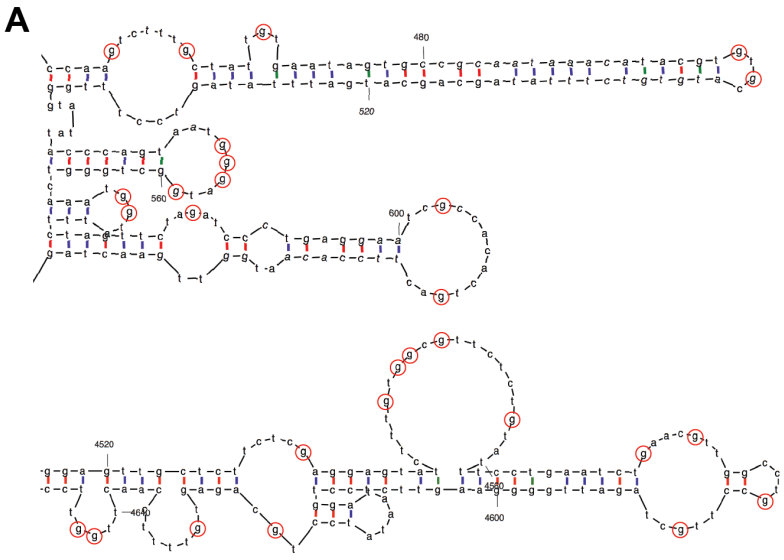
A

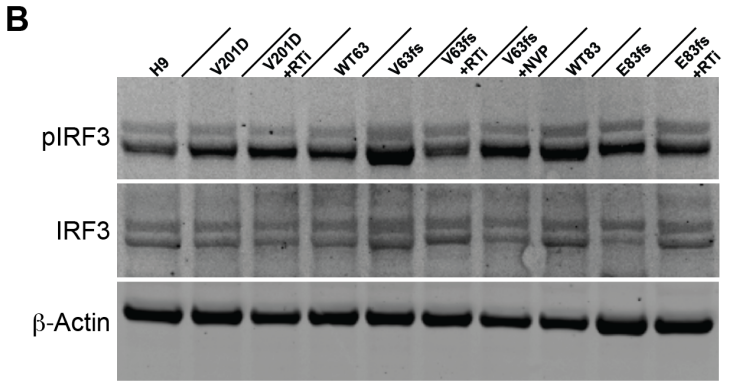
B
H9
V201D
V201D +RTi
WT63
V63fs
V63fs +RTi
V63fs +NVP
WT83
E83fs
E83fs +RTi
pIRF3
IRF3
β-Actin

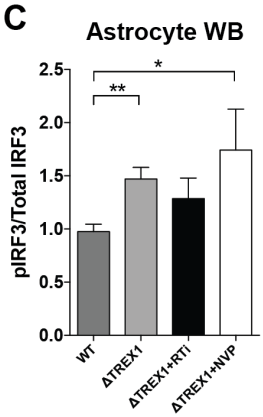
C
Astrocyte WB
pIRF3/Total IRF3
2.5
2.0
1.5
1.0
0.5
0.0
*
**
WT
ΔTREX1
ΔTREX1+RTi
ΔTREX1+NVP

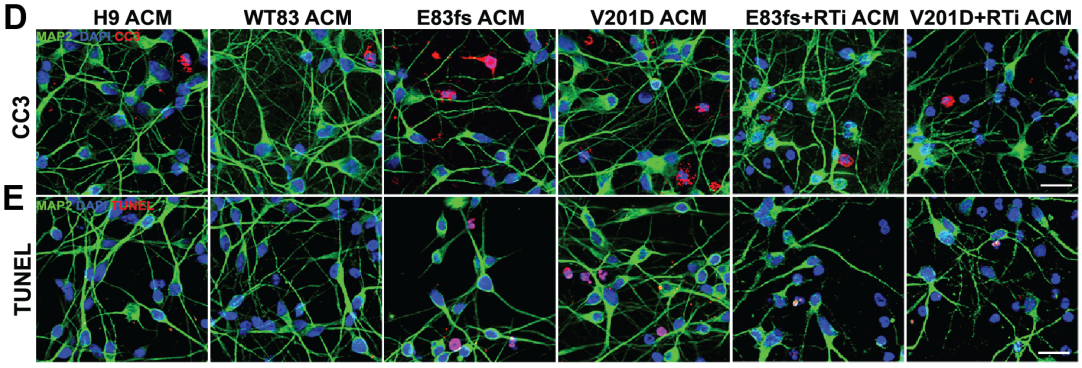
D
H9 ACM
WT83 ACM
E83fs ACM
V201D ACM
E83fs+RTi ACM
V201D+RTi ACM
MAP2 DAPI CC3
CC3
E
MAP2 DAPI TUNEL
TUNEL

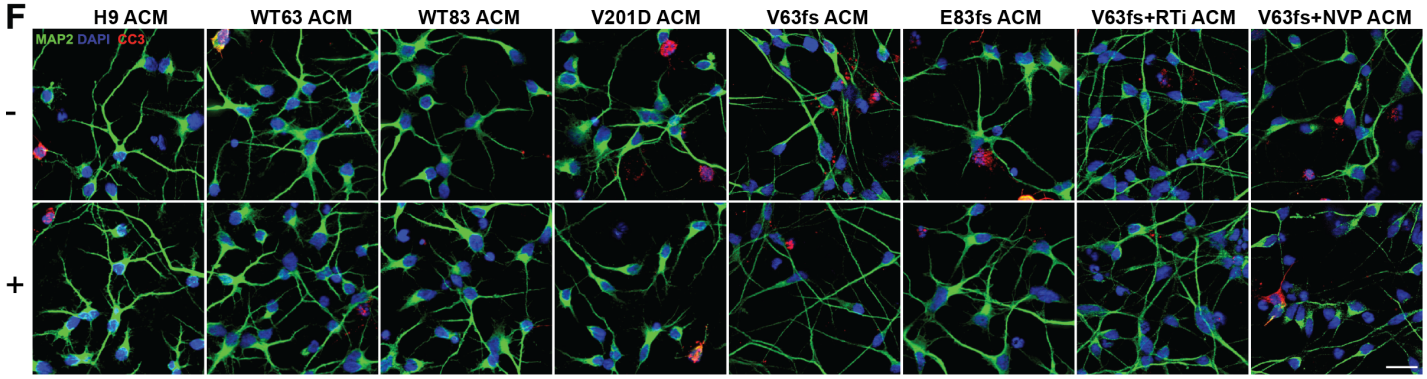
F
H9 ACM
WT63 ACM
WT83 ACM
V201D ACM
V63fs ACM
E83fs ACM
V63fs+RTi ACM
V63fs+NVP ACM
MAP2 DAPI CC3
-
+

Figure S6

**Supplemental Figure Legends:**

**Figure S1. Related to Figure 1 | Generation and mutation analysis of human pluripotent cell lines devoid of TREX1 function**. **A**, Dot plots showing the eGFP expression of the Cas9-2A-eGFP vector used in conjunction with guide RNA (gRNA) to mutagenize the *TREX1* locus in H9 ESCs. **B**, Surveyor nuclease activity of genomic DNA extracted from H9 ESCs following FACs. The PCR product was 538 bp long. The cleavage sites for gRNA1 and gRNA2 were 266 bp and 327 bp from the 5' end of the PCR product, respectively. **C**, Summary of exome sequencing across the V63 and E83 loci. The inserted nucleotides causing the frame-shifts are marked in red. Numbers indicate the numbers of reads across the locus. **D**, Expression of *TREX1* in neural precursor cells determined via qPCR. Expression was normalized to zero. *B2M* and *HPRT1* were used as dual internal references. **E**, Representative immunofluorescence images of the pluripotent markers Lin28 and Nanog. Scale bar, 200μm. **F**, Expression of pluripotent markers determined via qPCR. Expression was normalized to zero, and *HPRT1* was used as an internal reference. **G**, Hematoxylin and eosin staining of teratomas. All three germ layers are present. **H,** Karyotypes of the TREX1-deficient cell lines.

**Figure S2. Related to Figure 1 | Differentiation of pluripotent cell lines into neural cells**. **A**, Phase-contrast images outlining the NPC differentiation protocol. Pluripotent stem cells (PSCs) were grown as colonies until they became large, and they were then lifted to form embryoid bodies (EBs). Embryoid bodies were grown in suspension on a shaker until plating, after which rosettes formed. Rosettes were picked and dissociated to form neural precursor cells (NPCs). Scale bars in μm, as indicated within each panel. **B**, Phase-contrast images outlining neuronal differentiation. For neuronal differentiation, bFGF was removed from the NPC media. After 21 days, neurons were purified via FACS. **C**, Dot plot of the FACs purification of neurons. Neurons were collected by selecting for $CD184^{-}$ $CD44^{-}$ $CD24^{+}$ cells. **D**, Phase-contrast images outlining astrocyte differentiation. For astrocytic differentiation, the NPCs were lifted to form neurospheres and then grown in suspension with and pushed towards astrocytes. After 21 days, the neurospheres were plated, and the astrocytes proliferated, growing out of the spheres. The astrocytes were collected and propagated. Scale bar in μm, as indicated within. **E**, Fluorescent images corroborating astrocyte differentiation using a GFAP::GFP lentiviral construct. **F**, Representative immunofluorescence images of the NPC markers Nestin and SOX2. Scale bar, 20μm. **G**, Expression of NPC markers determined via qPCR. Expression was normalized to zero, and *B2M* and *HPRT1* were used as dual internal references. **H**, Representative immunofluorescence images of the neuronal markers MAP2 and Synapsin. Scale bar, 20μm. **I**, Expression of neuronal markers determined via qPCR. Expression was normalized to zero, and *B2M* and *HPRT1* were used as dual internal references. **J**, Representative immunofluorescence images of the astrocytic markers GFAP and S100. Scale bar, 20μm. **K**, Expression of astrocyte markers determined via qPCR. Expression was normalized to zero, and *B2M* and *HPRT1* were used as dual internal references. The presented values are the means ± SD.

**Figure S3. Related to Figure 1 | Validation of ssDNA antibody and quantification of ssDNA in TREX1-deficient cells. A**, Immunofluorescence of ssDNA in NPCs transfected with increasing amounts of single-stranded oligonucleotides. **B**, Immunofluorescence image of ssDNA in oligo-transfected and S1-treated NPCs. **C**, Immunofluorescence image of ssDNA or dsDNA in TREX1-deficient NPCs.

Scale bar, 20μm. **D**, Representative immunofluorescence images of ssDNA in fibroblasts. **E**, Graphical representation of ssDNA puncta levels in wild-type and AGS fibroblasts. **F**, Representative immunofluorescence images of ssDNA in PSCs. **G** Graphical representation of ssDNA puncta levels in wild-type and TREX1-deficient PSCs. **H**, Representative immunofluorescence images of ssDNA in NPCs. **I**, Graphical representation of ssDNA puncta levels in each NPC line. **J**, Representative immunofluorescence images of ssDNA in NPCs. Lentivirus expressing human *TREX1* was transduced into the V63fs line. **K**, Graphical representation of ssDNA puncta levels in WT63, V63fs, and V63fs transduced with lentivirus expressing human *TREX1*. **L**, Representative immunofluorescence images of ssDNAs in neurons. **M**, Graphical representation of ssDNA puncta levels in neurons from each line. **N**, Representative immunofluorescence images of ssDNAs in astrocytes. **O**, Graphical representation of ssDNA puncta levels in astrocytes from each line. Each dot represents one cell. Bars depict the means ± SD. Scale bar, 20μm. **P,** Normalized ssDNA puncta density across different stages of neural differentiation. The presented values are the means ± SEM.

**Figure S4. Related to Figure 2 | TREX1 deficiency results in increased levels of L1 but not Alu in the extrachromosomal fraction. A**, Representative graphs depicting the species identified in the extrachromosomal fraction by deep sequencing. The WT63, V63fs, and V63fs+RTi extrachromosomal fractions were sequenced. The results from the V63fs line are shown. **B**, Relative proportions of each mobile element's representation in the human genome. **C**, Composition of DNA species in the extrachromosomal fraction as determined by deep sequencing. Mitochondrial and non-repetitive DNA were excluded. **D**, Composition of L1 subfamilies in the extrachromosomal fraction as determined by deep sequencing. **E,** Schematic of *L1Hs* gene with bars representing mapping of sequencing reads. **F**, Relative quantity of Alu species in the extrachromosomal fraction, as determined by deep sequencing (n = 1; n = cell line). **G**, Relative mitochondrial DNA levels, as indicated by the *7S* gene and determined via qPCR. Quantities relative to NPC gDNA. **H**, Relative quantities of AluY and AluS in the extrachromosomal fraction. Hirt DNA was acquired in duplicate from each NPC cell line and normalized to the cell number at the time of extrachromosomal DNA extraction. The quantities from each extraction were averaged and graphed according to genotype (n = 6). Mutant lines were chronically treated with RTi (n = 6) or NVP (n = 2). The presented values are the means ± SD. Student's t-tests with Welch's correction were performed to compare genotypes. **I**, Western blot showing reduced expression of L1 ORF1p relative to β–actin after shRNA knockdown of LINE-1. **J**, Quantification of L1 mRNA expression in WT and TREX1-deficient NPCs relative to fibroblasts. **K**, Quantification of L1 mRNA expression in WT and TREX1-deficient neurons relative to fibroblasts. **L**, Quantification of L1 mRNA expression in WT and TREX1-deficient astrocytes relative to fibroblasts. The presented values are the means ± SEM**. M**, Representative FACS plots showing cells with *de novo* retrotransposition events (P3, $FITC^+$) in WT or TREX1-deficient NPCs transfected with p99-GFP-LRE3-mCherry retrotransposition reporter construct (P5, $PE^+$).

**Figure S5. Related to Figure 3 and Figure 4 | TREX1-deficient fibroblasts, PSC, NPCs, and neurons have no increase in toxicity compared to wild-type controls. A**, Representative immunofluorescence images of cleaved caspase-3 in purified neurons of different genotypes. **B**, Representative immunofluorescence images of TUNEL staining in purified neurons of different genotypes. **C**, Representative images of CC3 staining in WT and AGS fibroblasts. **D**,

Representative images of CC3 staining in WT and TREX1-deficient PSCs. **E**, Graphical representation of the percentages of NPCs positive for cleaved caspase-3. The presented values are the means ± SD (n = 3) (RTi, n = 3) (NVP, n = 1) (n=cell lines). Student's t-test with Welch's correction revealed no significant difference between the TREX1-deficient and control lines. **F,** Graphical representation of the percentages of astrocytes positive for cleaved caspase-3. The presented values are the means ± SD (n = 3) (RTi, n = 3) (NVP, n = 1) (n=cell lines). Student's t-test with Welch's correction revealed no significant difference between the TREX1-deficient and control lines. **G,** Images of immunostaining showing presence of neural cells and stratification of cell populations within wild-type 3D organoids. Scale bar, 200μm. **H**, Histogram showing distribution of organoids for each genotype/treatment after neuronal maturation. **I**, Representative images of CC3 staining in organoids showing apoptosis occurring primarily in $MAP2^+$ neurons (located outside of the proliferative region circled by dotted line). Scale bars, 50μm.

**Figure S6. Related to Figure 5 and Figure 6 | TREX1 deficiency results in neurotoxicity that is further exacerbated by TREX1-deficient astrocytes via type-I IFNs.** **A**, Representative potentially immunogenic Y-form secondary structures of L1Hs reverse-transcribed ssDNA containing unpaired guanosine nucleotides. **B**, Western blot detecting pIRF3, IRF3, and β-actin in astrocytes. **C**, Quantification of ratio between pIRF3 and total IRF3, normalized to V63fs (n = 5) (RTi, n = 4) (NVP, n = 3). **D,E,** Immunofluorescence images of cleaved caspase-3 (**D**) and TUNEL (**E**) in purified H9 neurons overlaid with astrocyte-conditioned media from different genotypes. Scale bars, 20μm. **F**, Representative images of CC3 and images of H9 purified neurons overlaid with astrocyte-conditioned media of different genotypes with or without the addition of IFNAR2 neutralizing antibody, along with corresponding graphs (n = 3). The V63fs mutant line was chronically treated with RTi, and RTi was removed during media conditioning (n = 1). The V63fs line was chronically treated with NVP, and NVP was removed during media conditioning (n = 1; n = cell lines). Scale bar, 20μm.